



HAL
open science

Tracing the origin of suspended sediment in a large Mediterranean river by combining continuous river monitoring and measurement of artificial and natural radionuclides

Mathilde Zebracki, Frédérique Eyrolle-Boyer, O. Evrard, David Claval, Brice Mourier, Stéphanie Gairoard, Xavier Cagnat, Christelle Antonelli

► To cite this version:

Mathilde Zebracki, Frédérique Eyrolle-Boyer, O. Evrard, David Claval, Brice Mourier, et al.. Tracing the origin of suspended sediment in a large Mediterranean river by combining continuous river monitoring and measurement of artificial and natural radionuclides. *Science of the Total Environment*, 2015, 502, pp.122-132. 10.1016/j.scitotenv.2014.08.082 . hal-01085335

HAL Id: hal-01085335

<https://sde.hal.science/hal-01085335>

Submitted on 18 May 2020

HAL is a multi-disciplinary open access archive for the deposit and dissemination of scientific research documents, whether they are published or not. The documents may come from teaching and research institutions in France or abroad, or from public or private research centers.

L'archive ouverte pluridisciplinaire **HAL**, est destinée au dépôt et à la diffusion de documents scientifiques de niveau recherche, publiés ou non, émanant des établissements d'enseignement et de recherche français ou étrangers, des laboratoires publics ou privés.

1 **Tracing the origin of suspended sediment in a large Mediterranean**
2 **river by combining continuous river monitoring and measurement of**
3 **artificial and natural radionuclides**

4
5
6 5 Mathilde Zebracki^{1*}, Frédérique Eyrolle-Boyer¹, Olivier Evrard², David Claval¹, Brice
7 6 Mourier^{3,4}, Stéphanie Gairoard⁵, Xavier Cagnat⁶, Christelle Antonelli¹

8 8 ¹Laboratoire d'Etudes Radioécologiques en milieu Continental et Marin (LERCM), Institut
9 9 de Radioprotection et de Sûreté Nucléaire (IRSN), Saint-Paul-lez-Durance, France

10 10 ²Laboratoire des Sciences du Climat et de l'Environnement (LSCE/IPSL), Unité Mixte
11 11 de Recherche 8212 (CEA/CNRS/UVSQ), Gif-sur-Yvette, France

12 12 ³Université Lyon 1, UMR 5023 Ecologie des Hydrosystèmes Naturels et Anthropisés,
13 13 ENTPE, CNRS, 3, Rue Maurice Audin, F-69518 Vaulx-en-Velin, France

14 14 ⁴Université de Limoges, GRESE, EA 4330, 123 avenue Albert Thomas, 87060
15 15 Limoges, France

16 16 ⁵Centre de Recherche et d'Enseignement de Géosciences de l'Environnement
17 17 (CEREGE), Unité Mixte 34 (AMU/CNRS/IRD), Aix-en-Provence, France

18 18 ⁶Laboratoire de Mesure de la Radioactivité dans l'Environnement (LMRE), Institut
19 19 de Radioprotection et de Sûreté Nucléaire (IRSN), Orsay, France

20 20 *Corresponding author: zebracki@free.fr

21
22 22 **ABSTRACT**

23 23 Delivery of suspended sediment from large rivers to marine environments has
24 24 important environmental impacts on coastal zones. In France, the Rhone River
25 25 (catchment area of 98,000 km²) is by far the main supplier of sediment to the
26 26 Mediterranean Sea and its annual solid discharge is largely controlled by flood
27 27 events. This study investigates the relevance of alternative and original
28 28 fingerprinting techniques based on the relative abundances of a series of
29 29 radionuclides measured routinely at the Rhone River outlet to quantify the relative
30 30 contribution of sediment supplied by the main tributaries during floods. Floods
31 31 were classified according to the relative contribution of the main subcatchments
32 32 (i.e., Oceanic, Cevenol, extensive Mediterranean and generalised). Between 2000
33 33 and 2012, 221 samples of suspended sediment were collected at the outlet and
34 34 were shown to be representative of all flood types that occurred during the last

35 decade. Three geogenic radionuclides (i.e., ^{238}U , ^{232}Th and ^{40}K) were used as
36 fingerprints in a multivariate mixing model in order to estimate the relative
37 contribution of the main subcatchment sources - characterised by different
38 lithologies - in sediment samples collected at the outlet. Results showed that total
39 sediment supply originating from Pre-Alpine, Upstream, and Cevenol sources
40 amounted to 10, 7 and $2 \cdot 10^6$ tons, respectively. These results highlight the role of
41 Pre-Alpine tributaries as the main sediment supplier (53 %) to the Rhone River
42 during floods. Other fingerprinting approaches based on artificial radionuclide
43 activity ratios (i.e., $^{137}\text{Cs}/^{239+240}\text{Pu}$ and $^{238}\text{Pu}/^{239+240}\text{Pu}$) were tested and provided a
44 way to quantify sediment remobilisation or the relative contributions of the
45 southern tributaries. In future, fingerprinting methods based on natural
46 radionuclides should be further applied to catchments with heterogeneous
47 lithologies. Methods based on artificial radionuclides should be further applied to
48 catchments characterised by heterogeneous post-Chernobyl ^{137}Cs deposition or by
49 specific releases of radioactive effluents.

50 1 Introduction

51 Delivery of suspended sediments from large rivers to marine environments has
52 important environmental impacts on coastal zones, where it modifies water
53 quality, estuarine geomorphology and biogeochemical cycles (Syvitski et al. 2005;
54 Meybeck and Vörösmarty 2005; Meybeck et al. 2007; Durrieu de Madron et al.
55 2011). Furthermore, the quality of riverine suspended sediment is impacted by
56 human activities in the river catchment, and sediments may transport various
57 particle-reactive contaminants from their sources within the catchment and convey
58 them into marine environments (Durrieu de Madron et al. 2011; Fohrer and
59 Chicharo 2011).

60 The magnitude of this impact is controlled by the sediment discharge of rivers that
61 is strongly variable throughout time (Meybeck et al. 2003). In France, the Rhone
62 River is by far the main supplier of sediment to the marine environment (Delmas et
63 al. 2012).

64 The Rhone River supplies almost two-thirds of the total river discharge into the
65 western Mediterranean Sea (Ludwig et al. 2009), delivering together with the Po
66 River the most important input of suspended sediment to the Mediterranean Sea
67 (Syvitski and Kettner 2007). It delivers more than 80 % of the particulate inputs to

68 the Gulf of Lions (Raimbault and Durrieu de Madron 2003) and exerts thereby a
69 major ecological influence by enhancing primary productivity (Bosc et al. 2004).
70 In the Rhone River, export of annual suspended solid loads is concentrated during
71 floods (Sempéré et al. 2000; Ollivier et al. 2011) with significant inputs from
72 southern tributaries (Pont et al. 2002). For instance, the large flood that occurred
73 in December 2003 exported 83 % of the total annual sediment load (Antonelli et
74 al., 2008; Ollivier et al. 2010). As it covers a large drainage area (98,000 km²)
75 characterized by strong variations in climate and geological conditions, the relative
76 contribution of the main Rhone River tributaries to its sediment discharge may vary
77 throughout time (Pardé, 1925; Pont et al. 2002; Antonelli et al. 2008). Sediment
78 conveyed by the Rhone River was documented to contain large concentrations in
79 contaminants, such as organic pollutants (Sicre et al., 2008; Desmet et al. 2012;
80 Mourier et al. 2014) and metals (Radakovitch et al. 2008). In addition, the Rhone
81 valley represents Europe's largest concentration of nuclear power plants, and the
82 river receives radioactive liquid effluents originating from four nuclear plants and a
83 spent fuel reprocessing plant currently under dismantlement. As a consequence,
84 sedimentary archives were shown to reflect significant enrichments in artificial
85 radionuclides in the lower Rhone River sections (Ferrand et al. 2012). It is
86 therefore crucial to better constrain those sources as marine sediments have the
87 capacity to store these contaminants in continental shelf areas and in abyssal
88 plains (Charmasson et al. 1998; Radakovitch et al. 1999; Lee et al. 2003; Garcia-
89 Orellana et al. 2009).

90
91 In this context, quantifying the sources supplying sediments to the Rhone River and
92 eventually to the Mediterranean Sea represents a crucial prerequisite for better
93 understanding the riverine transfer and its potential role in global biogeochemical
94 cycles, and for implementing effective control strategies to improve water and
95 sediment quality (Walling and Collins 2008). The relative contribution of sediments
96 originating from the main tributaries during the floods recorded in the lower
97 sections of the Rhone River was shown to reflect lithological differences and to
98 imprint the geochemical and mineralogical properties of the main upstream
99 sediment sources (Pont et al. 2002; Ollivier et al. 2010; Zebracki et al. 2013a). We

100 therefore propose to use these sediment characteristics to fingerprint the origin of
101 sediment transported in the lower Rhone River.

102

103 Exports of suspended sediments from the Rhone River have been continuously
104 monitored since 2000 at the Rhone River Observatory Station in Arles (SORA), which
105 is located 40 km upstream of its mouth. Furthermore, the suspended sediment
106 content in natural and artificial radionuclides has been continuously analysed in
107 the framework of legal radioecological surveillance (Eyrolle et al., 2012).

108

109 This study therefore proposes to provide alternative and original fingerprinting
110 techniques based on radionuclide properties measured routinely to quantify the
111 proportion of sediments supplied by the different tributaries to the Rhone River
112 outlet during floods. Variations in geogenic ^{238}U , ^{232}Th and ^{40}K radionuclide
113 activities may reflect the contribution of source areas with different lithologies
114 (Olley et al. 1993; Yeager and Santschi 2003). In addition, among artificial
115 radionuclides, spatial variations in ^{137}Cs and plutonium isotope activities (i.e., ^{238}Pu
116 and $^{239+240}\text{Pu}$) may provide powerful tracers of the sediment origin. During Rhone
117 River floods, ^{137}Cs was shown to originate mainly from erosion of the soils
118 contaminated by global atmospheric fallout and Chernobyl accident (Antonelli et
119 al. 2008), and to display an East-West decreasing gradient of contamination across
120 the catchment (Renaud et al. 2003; Roussel-Debel et al. 2007). In contrast, and in
121 the particular case of the lower Rhone River, Pu isotopes may either originate from
122 erosion of the catchment soils contaminated by global atmospheric fallout or from
123 remobilisation of sediment labeled by liquid effluents released by the Marcoule
124 spent fuel reprocessing plant (from 1960s and decommissioned since 1997).

125 A method based on $^{238}\text{Pu}/^{239+240}\text{Pu}$ activity ratio (PuAR) measurements was
126 developed to estimate the fraction of the Pu isotopes that originated from the
127 Rhone River in marine deposits (Thomas 1997; Lansard et al. 2007). This method
128 was applied to distinguish between Pu supply through soil erosion across the Rhone
129 catchment and remobilisation of sediment stored in the river channel downstream
130 of Marcoule, and to quantify their relative contribution to Pu fluxes recorded at
131 Arles (Rolland 2006; Eyrolle et al. 2012).

132

133 After identifying the origin of floods, fingerprinting techniques presented above
134 were applied to quantify the relative contribution of the main sources delivering
135 sediments to the Rhone River, based on the continuous measurement of natural
136 and artificial radionuclides. They were applied to suspended sediments collected at
137 Arles outlet (SORA observatory station) between October 2000 and June 2012.

138 **2 Study area**

139 The Rhone River basin area consists of four mountainous subcatchments, i.e., Alps,
140 Jura, Cevennes/Massif Central, and Vosges. In the northern part of the basin, the
141 Jura and Vosges mountains (drained by the Saone River) are mainly calcareous.
142 When moving to the South and to the East, the Alpine mountains (drained by the
143 Upper Rhone, Isere and Durance rivers) mostly consist of sedimentary rocks and of
144 siliceous crystalline and metamorphic rocks. Finally, in the southwestern part of
145 the basin, crystalline siliceous rocks dominate in the Cevennes Mountains (drained
146 by the Ardeche, Ceze and Gard rivers). Details on those geological substrate
147 variations are given in Ollivier et al. 2010 and Ollivier et al. 2011. In addition to
148 this geological heterogeneity, the Rhone basin is exposed to a wide variety of
149 climate conditions (Pont et al. 2002). The tributaries of the Rhone are used to be
150 organized in three main groups characterised by distinct hydrographic features
151 (Figure 1): northern tributaries (Ain, Fier, Isere, Saone rivers) and southern
152 tributaries, which may in turn be distinguished as Cevenol tributaries (Eyrieux,
153 Ardeche, Ceze, Gard rivers) and southern Pre-Alpine tributaries (Durance, Drome,
154 Aigues, and Ouveze rivers).

155 Forty kilometres upstream of its mouth the Rhone River subdivides into the Grand
156 Rhone River and the Petit Rhone River, and flows into a delta of 1 500 km² (Figure
157 1). The sampling station in Arles is located on the Grand Rhone River, which drains
158 about 90 % of the water discharge. The SORA observatory in Arles is an automatic
159 sampling station operated by the French Institute for Radioprotection and Nuclear
160 Safety (IRSN/LERCM).

161 At the Beaucaire gauging station (i.e., 8 km upstream of the Rhone diffluence, and
162 14 km upstream of the SORA sampling station in Arles), the Rhone mean annual
163 discharge was about 1,700 m³.s⁻¹ for the period 1920-2012, while the annual
164 suspended solid load varied from 1.2 to 19.7 Mt.yr⁻¹ for the period 1961-1996
165 (Antonelli 2002; Pont et al. 2002). River discharges associated with the 1-yr, 2-yr,

166 10-yr, and 100-yr return periods amount to 4,000, 5,000, 8,400 and 11,200 m³.s⁻¹,
167 respectively.

168 **3 Materials and methods**

169 **3.1 Flood classification**

170 Based on the previous description of the flood types (Parde 1925), four types of
171 climatological regimes are distinguished (Figure 1):

172 (1) Oceanic floods generally occurring in winter and resulting from rainfall in
173 the northern part of the basin (Fier, Ain, Isere, Saone rivers);

174 (2) Cevenol floods occurring mainly in autumn and resulting from flash-flood
175 type storms affecting the southwestern tributaries of the Rhone River
176 (Ardeche, Ceze, Gard, Eyrieux rivers);

177 (3) Extensive Mediterranean floods resulting from precipitations affecting the
178 right bank area of the river (Cevenol tributaries listed above) and the sub-
179 Alpine tributaries located on the left bank of the Rhone River (Durance,
180 Ouveze West Bank, Aigues rivers as well as to a lesser extent the Drome
181 River);

182 (4) Generalized floods mostly occurring in autumn and affecting both northern
183 and southern tributaries.

184 During the period 2000-2012, water discharge data recorded at Arles gauging
185 station and downstream of the twelve tributaries mentioned above were provided
186 by the *Compagnie Nationale du Rhône* (CNR).

187 Flood classification was performed by comparing the rise in water discharge
188 registered at the Rhone River monitoring station during sampling to the
189 hydrographs of the relevant upstream tributaries (according to the method
190 described by Pont et al. 2002, Rolland 2006, and Antonelli et al. 2008).

191 Flood classification was refined by considering the mean maximal daily water
192 discharge recorded during floods (Zebracki et al. 2013b) to discriminate between
193 small-scale floods (3,000-4,000 m³.s⁻¹), intermediate floods (4,000-5,000 m³.s⁻¹),
194 large-scale floods (5,000-9,000 m³.s⁻¹), and exceptional floods (> 9,000 m³.s⁻¹).

195 **3.2 Suspended sediment sampling procedures during flood events**

196 **3.2.1 Particle-associated radionuclides**

197 Sampling procedures during periods of high water discharge (> 3,000 m³.s⁻¹) are
198 detailed in Eyrolle et al. 2012. Briefly, since 2005, 5 L water samples were

199 collected every 20 minutes and directly filtered onto 0.5 µm Milligard® cellulose
200 acetate cartridges. The filter clogging was continuously monitored, so that the
201 filtration was stopped when 50 % of clogging was achieved or after 8 hours.
202 Subsequent water samples were then collected on successive filters, which were
203 analysed separately. Before 2005, samples were manually collected during floods.
204 Additional suspended sediment samples were obtained either after filtering river
205 water through Milligard® cartridges or by decanting suspended matter contained in
206 at least 120 L river water samples.

207 3.2.2 Suspended sediment load

208 Sampling procedures during periods of high water discharge ($> 3,000 \text{ m}^3 \cdot \text{s}^{-1}$) are
209 detailed in Eyrolle et al. 2012. In summary, six suspended sediment samples were
210 collected daily to improve flood monitoring by collecting 150 mL every 30 min.
211 Before 2005, samples consisted of manual collection of river water at hourly time
212 step.

213 The suspended sediment load exported during floods was calculated from river
214 discharge and suspended sediment concentration records.

215 3.3 Radionuclide analyses on suspended sediment collected at Arles station

216 3.3.1 Gamma emitters

217 For gamma spectrometry analyses suspended sediment samples were ashed and put
218 into tightly closed plastic boxes for gamma counting (20-60 g) using low-background
219 and high resolution Germanium Hyper pure detectors at the IRSN/LMRE laboratory
220 in Orsay (Bouisset and Calmet 1997). For each sample, up to 29 gamma-emitting
221 radionuclides (both natural and artificial) were determined. Time between
222 sampling and analysis varied between 29 and 333 days, with a mean of 77 d.

223 In this study, we restricted the analysis to measurements of ^{40}K , ^{232}Th , ^{238}U (natural
224 radionuclides) and ^{137}Cs (artificial radionuclide). Due to their long-term radioactive
225 decay, the activities in ^{232}Th and ^{238}U were estimated by measuring the contents of
226 their short-lived filiation products, i.e., ^{228}Ac and ^{234}Th respectively, and assuming
227 secular equilibrium within the corresponding radioactive decay series. The use of
228 ^{228}Ac as a proxy to estimate ^{232}Th content in sediment relies on the assumption that
229 ^{228}Ra is not preferentially remobilised in the riverine system.

230 Efficiency calibrations were constructed using gamma-ray sources in a $1.15 \text{ g} \cdot \text{cm}^{-3}$
231 density solid resin-water equivalent matrix. Activity results were corrected for true

232 coincidence summing and self-absorption effects (Lefèvre et al. 2003). Measured
233 activities, expressed in Bq.kg⁻¹ dry weight, are decay-corrected to the date of
234 sampling. The activity uncertainty was estimated as the combination of calibration
235 uncertainties, counting statistics, and summing and self-absorption correction
236 uncertainties.

237 3.3.2 Alpha emitters

238 When available sample amount was sufficient (i.e., 50-200 g of dry matter),
239 analyses of plutonium isotopes (²³⁸Pu and ²³⁹⁺²⁴⁰Pu) were performed by alpha
240 spectrometry at IRSN/LMRE (Goutelard et al. 1998; Lansard et al. 2007). In brief,
241 ashed samples were leached with nitric acid, co-precipitated and purified using
242 exchange resins before electro-deposition, and then counted on low background
243 PIPS® detectors for up to 14 days. The detection limit for the analytical procedure
244 was 1 mBq for both ²³⁸Pu and ²³⁹⁺²⁴⁰Pu.

245 3.4 Sediment sources natural radionuclides ²³⁸U, ²³²Th and ⁴⁰K contents

246 Based on the signatures of different lithological sources previously described for
247 the Rhone River basin (Pont et al., 2002; Ollivier et al., 2010), we identified three
248 main contrasting source areas, i.e., “Upstream”, “Pre-Alpine”, and “Cevenol”
249 sediment sources, corresponding to (1) the northern part of the Rhone basin
250 (mainly calcareous), (2) the southern-left bank of the river (sedimentary rocks),
251 and (3) the southern-right bank area (crystalline siliceous rocks).

252 Natural radionuclide contents in these three sediment sources were assessed based
253 on a set of available fine-grained sediment samples (Figure 1). Radionuclide
254 composition of the southern-right bank source was measured in suspended material
255 transported during flood events recorded on the Ardeche, Ceze and Gard Rivers in
256 December 2003 (Rolland 2006), November 2011 and November 2012. Radionuclide
257 composition of the southern-left bank originating sediment was measured on the
258 sediment core layers that were estimated to have deposited between 2000 and
259 2009 at the outlet of the Bleone River, i.e., the main tributary of the Durance River
260 (Navratil et al., 2012). Radionuclide properties of the third sediment source area,
261 i.e., the upstream tributaries flowing into the Rhone River upstream of the Cevenol
262 tributaries, were assessed by using a sediment core collected in 2011 in the so-
263 called “Grange Ecrasee” secondary channel of the Rhone River, ca. 15 km upstream
264 of its confluence with the southern tributaries (Mourier et al. 2014). Sediment core

265 layers were collected in low water flow conditions that allowed for sediment
266 deposition. The collected sediment was characterised by the dominance of silt- and
267 clay-sized material (i.e. < 63 µm; 80 % of material in the Bleone River core, and
268 73 % in the Grange Ecrasee core). Unfortunately, grain size composition of
269 suspended sediment collected in the framework of continuous radiological
270 monitoring was not measured routinely, but available measurements show that this
271 material is fine-grained and that the clay and silt fractions are dominant (Antonelli
272 et al. 2008). Direct comparison of radionuclide activities measured in both
273 subcatchment source material and in riverine suspended sediment was therefore
274 considered to be relevant and meaningful (e.g., Navratil et al. 2012).

275 ***3.5 Fingerprinting the sources delivering suspended sediment to the Lower Rhone River***

276 **3.5.1 Based on natural radionuclides ^{238}U , ^{232}Th and ^{40}K**

277 The natural radionuclide composition in ^{238}U , ^{232}Th and ^{40}K of the three sediment
278 sources (i.e., Upstream, Cevenol, Pre-Alpine) was assessed based on radionuclide
279 measurements in sediments representative of each subcatchment source. The
280 ability of these geogenic fingerprints to discriminate between the potential
281 sediment sources was assessed by conducting a range test (i.e., radionuclide
282 activities of suspended sediments discharged at the outlet of the Rhone River were
283 comprised in the range of values defined by those of the three sediment sources),
284 and by a non-parametric Kruskal-Wallis H -test (Collins and Walling 2002). The set
285 of the three geogenic radionuclides ^{238}U , ^{232}Th and ^{40}K successfully passed the
286 Kruskal-Wallis H -test. By performing a stepwise selection procedure, the
287 combination of the three geogenic radionuclides provided a good discrimination of
288 the different sources as they were associated with low Wilk's lambda values. A
289 multivariate mixing model was then used to estimate the relative contribution of
290 the potential sediment sources in each outlet sediment sample. By assuming a
291 normal distribution for each fingerprinting property and source, a series of 10,000
292 random positive numbers was generated from these distributions and used to
293 estimate the relative contribution of the potential sources in the sediment
294 samples. The robustness of the source ascription solutions were assessed using a
295 mean "goodness of fit" (GOF) index (Motha et al. 2003). Only the sets of simulated
296 random numbers that obtained a GOF index value higher than 0.80 were used in
297 the subsequent steps. The use of the Monte Carlo method allowed the calculation

298 of 95 % confidence intervals. The outputs of the mixing model appeared to be very
299 stable, all outputs being very close (and systematically within a range of ± 2 %) to
300 their mean value. It was therefore decided to present only those mean values in
301 the remainder of the text.

302 A detailed description of these procedures is provided in Evrard et al. (2011) and
303 Haddadchi et al. (2013).

304 3.5.2 Based on artificial radionuclides ^{137}Cs , ^{238}Pu and $^{239+240}\text{Pu}$

305 3.5.2.1 $^{238}\text{Pu}/^{239+240}\text{Pu}$ Activity ratio (Pu AR)

306 From analyses performed on French riverine sediments collected between 2003 and
307 2005, the $^{238}\text{Pu}/^{239+240}\text{Pu}$ activity ratio (Pu AR) characterizing the global
308 atmospheric fallout was estimated to 0.036 ± 0.006 (Eyrolle et al. 2008), whereas
309 the Marcoule radioactive liquid releases are characterized by a theoretical constant
310 Pu AR of 0.3 (Lansard et al. 2007). Within the river section located downstream of
311 Marcoule and assuming that no direct release of Pu occurs when water discharge
312 exceeds $4,000 \text{ m}^3 \cdot \text{s}^{-1}$ (Rolland 2006), Pu isotope contents in suspended sediment
313 result from the mixed contribution of erosion of soils of the Rhone catchment and
314 remobilisation of sediment deposits labeled by the Marcoule radioactive releases.
315 At the monitoring station in Arles, based on activity measurements in ^{238}Pu and
316 ^{239}Pu of suspended sediment, samples display Pu AR values corresponding to the
317 mixing of both sources (Eq. 2):

$$318 \frac{{}^{238}\text{Pu}_{\text{Sample}}}{{}^{239+240}\text{Pu}_{\text{Sample}}} = \frac{{}^{238}\text{Pu}_{\text{Marcoule}} + {}^{238}\text{Pu}_{\text{Catchment}}}{{}^{239+240}\text{Pu}_{\text{Marcoule}} + {}^{239+240}\text{Pu}_{\text{Catchment}}} \quad (2)$$

319
320 The fractions of the total Pu isotopes that were discharged at Arles and the ones
321 that were derived from sediment remobilisation ($^{238}\text{Pu}_{\text{Sed}}$ and $^{239+240}\text{Pu}_{\text{Sed}}$, in
322 percentage) are quantified using the following relationships (Eq. 3 and 4):

$$323 {}^{239+240}\text{Pu}_{\text{Sed}} = \frac{\text{PuAR}_{\text{Sample}} - \text{PuAR}_{\text{Catchment}}}{\text{PuAR}_{\text{Marcoule}} - \text{PuAR}_{\text{Catchment}}} \times 100 \quad (3)$$

$$324 {}^{238}\text{Pu}_{\text{Sed}} = {}^{239+240}\text{Pu}_{\text{Sed}} \times \frac{\text{PuAR}_{\text{Marcoule}}}{\text{PuAR}_{\text{Sample}}} \quad (4)$$

325 The uncertainty associated with each contribution was constrained by the standard
326 analytical deviation.

327 3.5.2.2 $^{137}\text{Cs}/^{239+240}\text{Pu}$ Activity ratio (Cs/Pu AR)

328

329 3.5.2.2.1 Cs/Pu AR in soils of the Rhone basin

1 330 The ^{137}Cs contained in soils of the Rhone catchment originates from both the global
2
3 331 atmospheric fallout (nuclear weapons testing from 1945 to the beginning of 1980s)
4
5 332 and Chernobyl accident (1986). In contrast $^{239+240}\text{Pu}$ in the soils of the Rhone
6
7 333 catchment was exclusively supplied by the global atmospheric fallout as no
8
9 334 additional plutonium supply was detected in the environment in France after
10 335 Chernobyl accident (Renaud et al. 2007).

11 336

12
13
14 337 Total theoretical atmospheric deposition of ^{137}Cs on soils was previously mapped at
15
16 338 the scale of France by using two empirical relationships (Roussel-Debet et
17
18 339 al. 2007): the first one linking the mean annual amount of rainfall and the
19
20 340 cumulative deposition from 1945 to 1982 for fallout supplied by the atmospheric
21
22 341 nuclear weapon tests (Mitchell et al. 1990), and the second one associating the
23 342 activity levels measured in soils with the daily rainfall recorded just after
24
25 343 Chernobyl accident (Renaud et al. 2003).

26
27 344 Based on the $^{137}\text{Cs}/^{239+240}\text{Pu}$ activity ratio characteristic of the global atmospheric
28
29 345 fallout (e.g., Masson et al. 2010), and the available cartography of ^{137}Cs deposition
30
31 346 (Roussel-Debet et al. 2007), the spatial distribution of $^{137}\text{Cs}/^{239+240}\text{Pu}$ activity ratio
32 347 (Cs/Pu AR) was mapped at the scale of the Rhone basin and decay-corrected to
33
34 348 1/1/2010.

35
36 349 Although radiocaesium and plutonium are chemically dissimilar elements, it has
37
38 350 been shown that ^{137}Cs and $^{239+240}\text{Pu}$ originating from atmospheric fallout remained
39
40 351 fixed together in soils over decades, suggesting the absence of geochemical
41
42 352 fractionation (Hodge et al. 1996).

43 353 Based on values found in the literature, the theoretical Cs/Pu AR in the Rhone
44
45 354 basin was decay-corrected in order to match with the study period (2000-2012) and
46
47 355 displayed values within the range of 27-42 (Hodge et al. 1996; Cochran et al. 2000;
48
49 356 Le Roux et al. 2010).

50
51 357 The mean Cs/Pu AR was then calculated for each subcatchment of the Rhone basin.
52
53 358 Deviation in this theoretical Cs/Pu AR indicates the supply of additional
54
55 359 radionuclide contamination by other sources than the bomb fallout (Hodge et al.
56
57 360 1996; Turner et al. 2003; Antovic et al. 2012). In the Rhone basin, this additional
58 361 source originates from the Chernobyl fallout.

60 362 3.5.2.2.2 Cs/Pu AR in suspended sediments of the lower Rhone River

61
62
63
64
65

363 In suspended sediment exported at the outlet of Rhone River, ^{137}Cs and $^{239+240}\text{Pu}$
364 originate from two sources: the erosion of Rhone catchment soils and the liquid
365 radioactive releases from nuclear industries (the Marcoule spent fuel reprocessing
366 plant for $^{239+240}\text{Pu}$ and ^{137}Cs , and nuclear power plants for ^{137}Cs).

367 The contribution from waste facilities originates either from direct releases or from
368 sediment remobilisation processes. Releases from nuclear industries are submitted
369 to authorisation and liquid discharges are not allowed during periods of high water
370 discharge (threshold of $4,000 \text{ m}^3 \cdot \text{s}^{-1}$ at Arles gauging station [Rolland 2006]).

371
372 Contrary to $^{238}\text{Pu}/^{239+240}\text{Pu}$, no specific signature in $^{137}\text{Cs}/^{239+240}\text{Pu}$ of radioactive
373 liquid releases has been identified so far. Among the nuclear facilities, the
374 potential source of Pu is unique (Marcoule reprocessing plant), whereas there are
375 potentially various sources of ^{137}Cs . Based on annual data chronicles of ^{137}Cs and
376 $^{239+240}\text{Pu}$ released in the Rhone River between 1963 and 2003 (Eyrolle et al. 2005),
377 the Cs/Pu AR was assessed in order to characterise the Marcoule reprocessing plant
378 signature.

379
380 The $^{137}\text{Cs}/^{239+240}\text{Pu}$ activity ratio in sediments may be affected by the different
381 geochemical behaviour of both elements and by their various sediment-water
382 distribution coefficients (K_d). However, it was shown that both artificial
383 radionuclides were strongly fixed to particles in freshwater environments (Cochran
384 et al. 2000; Le Cloarec et al. 2007). Our interpretations of the Cs/Pu AR variations
385 therefore relied on the hypothesis that both elements displayed a similar behaviour
386 in this environment and that they were strongly particle-reactive.

387
388 The uncertainty associated with $^{137}\text{Cs}/^{239+240}\text{Pu}$ values was calculated based on the
389 standard analytical deviation.

390 3.5.3 Coupling artificial and natural radionuclides methods

391 The three potential sediment sources that were discriminated by the fingerprinting
392 method based on natural radionuclides were also characterised by their Cs/Pu AR.
393 By coupling the Cs/Pu AR characteristics to the relative contribution of sediment
394 sources that resulted from the fingerprinting method based on natural
395 radionuclides, we calculated the expected values of Cs/Pu AR (Cs/Pu AR exp) and

396 compared them to the calculated values of Cs/Pu AR resulting from radionuclide
397 measurements in suspended sediments (Cs/Pu AR SS).

398 **4 Results and discussion**

399 **4.1 Sample collection and flood classification**

400 Between October 2000 and June 2012, 221 samples were collected during floods at
401 Arles. Those suspended sediment samples were taken during 37 flood events and
402 document 85 % of the floods that were recorded at Arles station during this period
403 (Supplementary information Figure S1). During this study, floods were dominated
404 by the occurrence of small-scale floods (76 %), followed in decreasing importance
405 order by intermediate floods (11 %), large floods (8 %) and exceptional floods (5 %)
406 corresponding to two flood events that occurred during autumn in 2002 and during
407 winter in 2003.

408 All floods that occurred in the lower section of the Rhone River could be classified
409 according to the proposed scheme (Table 1) with the exception of two floods that
410 occurred in 2010 (September and March). Both floods were characterised by a
411 relatively low maximum 1-h water discharge ($< 3,100 \text{ m}^3 \cdot \text{s}^{-1}$) with no clear
412 evolution throughout time. However, the number of suspended sediment samples
413 collected during both floods (*i.e.* < 3 % of the total) is negligible compared to the
414 entire dataset available. Unclassified suspended sediment samples were therefore
415 removed from further analysis.

416 Generalised, Oceanic, Cevenol and extensive Mediterranean floods were
417 documented by 40, 23, 23 and 11 % of the samples, respectively. All the flood types
418 were well represented in the compiled database. This database is therefore
419 representative of the entire range of flood types that occurred during the last
420 decade.

421 **4.2 Fingerprinting based on natural radionuclides**

422 **4.2.1 Activities in ^{238}U , ^{232}Th , ^{40}K and sediment source characteristics**

423 Activities in ^{238}U , ^{232}Th and ^{40}K of suspended sediment collected in the lower Rhone
424 River show that they were influenced by the flood type (Figure 2). When comparing
425 ^{238}U , ^{232}Th and ^{40}K activities in suspended sediment according to the flood type,
426 Cevenol events displayed the highest median values of all parameters suggesting a
427 specific signature of southwestern tributaries (Figure 2).

428 Cevenol floods display a geogenic radionuclide signature distinct from the other
429 floods. This difference could not only be due to specific lithological characteristics
430 but also to preferential conditions of sediment transport, as these floods display
431 typical flash-flood characteristics and their source area is located at a shorter
432 distance from the outlet sampling station.

433
434 The difference observed in ^{238}U , ^{232}Th and ^{40}K activities among the three sediment
435 sources provided a sound physico-chemical basis to discriminate between their
436 respective contributions at the Rhone River basin scale (Table 2, Supplementary
437 information Tables S1, S2 and S3). As expected, the Cevenol granitic sediment
438 source displayed the most enriched composition in all three natural radionuclides,
439 whereas their activities were the lowest in calcareous Pre-Alpine sources. The
440 larger variations associated with parameters characterising the Cevenol source can
441 be attributed to the larger spatial heterogeneity of this potential sediment source.

442 4.2.2 Sediment source contribution

443 The contribution of each sediment source, i.e., Upstream, Cevenol and Pre-Alpine,
444 to suspended sediment conveyed during floods in the Lower Rhone River is
445 displayed in Figure 3.

446 Cevenol floods were characterised by the highest interquartile range (i.e.
447 difference between the third and first quartiles; Figure 3b), reflecting the highest
448 temporal variability of sediment supply during these typical “flash-flood” events.
449 The mean contribution of sediment from Upstream, Pre-Alpine and Cevenol sources
450 amounted to 31 %, 30 % and 39 % of the total sediment input to the outlet,
451 respectively (Figure 3b). Although Cevenol floods were of relatively short duration
452 (from a few hours to a few days), they supplied an equivalent amount of sediment
453 as the two other sources to the outlet at a decadal timescale.

454 During extensive Mediterranean, Oceanic and generalised floods (Figure 3acd), Pre-
455 Alpine and Upstream inputs supplied a mean of 38-53 % and 36-39 % of the total
456 Rhone sediment export, and were therefore the main sediment contributors.

457 When comparing Oceanic floods with other flood types (Figure 3), we may have
458 expected a significantly larger contribution of Upstream sediment. However, this
459 was not observed, suggesting that material eroded in the northern part of the
460 catchment may not reach the outlet (at Arles) rapidly enough to imprint its

461 signature on material conveyed downstream. Contrary to Cevenol floods, Oceanic
1 462 floods are characterised by a slow and regular rise in water discharge. Those
2
3 463 specific sediment transport conditions combined with the presence of numerous
4
5 464 dams in this upper catchment part likely resulted in the significant storage of
6
7 465 material in reservoirs (Pont et al. 2002; Ollivier et al. 2010).
8
9

10 466 **4.2.3 Sediment load contribution**

11 467 Suspended sediment load was determined for all floods documented between 2000
12
13 468 and 2012, with the exception of 4 events (Nov. 2000, March and April 2001, and
14
15 469 Nov. 2004) for which the number of samples was considered not to be sufficient, or
16
17 470 because of the lack of precision in the timing of sample collection. Fourteen
18
19 471 samples (6 % of the entire sample set) were associated with those floods and were
20
21 472 therefore removed from further analysis.

22 473 By summing individual sediment loads associated with successive samples, the total
23
24 474 amount of suspended sediment discharged during floods between 2000 and 2012
25
26 475 was estimated to 19.5×10^6 tons. This amount is underestimated as 30 % of flood
27
28 476 events could not be sampled or were not completely documented by the
29
30 477 monitoring. Furthermore, it should be reminded that the precision of solid flux
31
32 478 estimations is strongly dependent on the sampling of suspended sediment
33
34 479 concentration variations during the floods (Ollivier et al. 2010). The sediment flux
35
36 480 during floods could not be compared with the total sediment export to the sea
37
38 481 during the entire study period, as corresponding data were not available for low
39
40 482 water flow periods. A rough comparison with previous findings outlines the strong
41
42 483 variability of both inter- and intra-annual fluxes of sediment in the Rhone River
43
44 484 (Supplementary information Table S4).

45 485 The contribution of suspended sediment originating from each source is
46
47 486 represented in Figure 4a. The sediment supply from Pre-Alpine, Upstream, and
48
49 487 Cevenol sources was estimated to 10, 6.8 and 2.2×10^6 tons, respectively. The
50
51 488 sediment inputs from southern tributaries (i.e., Pre-Alpine and Cevenol) accounted
52
53 489 for 65 % of the total particulate flux, which is close to the results reported by Pont
54
55 490 et al. 2002 (i.e., 72 %, Supplementary information Table S4). Our results further
56
57 491 highlight the dominant role of Pre-Alpine tributaries (and especially the Durance
58
59 492 River) as the main sediment supply (53 %) to the Rhone during floods.
60
61
62
63
64
65

493 During generalised, extensive Mediterranean, Cevenol and Oceanic floods,
494 sediment export was estimated to 11, 6.4, 1.4 and 0.7×10^6 tons of sediment,
495 respectively (Figure 4b). Generalised and extensive Mediterranean floods thereby
496 deliver the bulk of the Rhone sediment to the sea (87 % of the total sediment
497 supply).

498 **4.3 Fingerprinting based on artificial radionuclides**

499 **4.3.1 Activity ratio $^{238}\text{Pu}/^{239+240}\text{Pu}$**

500 During floods, the calculated Pu AR activity ratio exceeded systematically the
501 reference value in the catchment soils (i.e., 0.036 ± 0.006 , see Table 3). This
502 reflects the continuous occurrence of remobilisation of Marcoule-labeled sediment
503 and confirms that sediment remobilisation provides a significant secondary source
504 of Pu to the Rhone River prodelta (Miralles et al. 2004; Eyrolle et al. 2006; Lansard
505 et al. 2007) and the offshore zone (Garcia-Orellana et al. 2009; Dufois et al. 2014).

506
507 At a given date, the contribution of ^{238}Pu originating from remobilised sediment
508 was systematically higher than the $^{239+240}\text{Pu}$ fraction (Table 3). In most cases,
509 sediment remobilisation was shown to act as the primary source of ^{238}Pu in
510 suspended sediment discharged by the Rhone River, whereas soil erosion in the
511 Rhone catchment provided the dominant source of $^{239+240}\text{Pu}$. The enrichment of
512 sediment in ^{238}Pu compared to $^{239+240}\text{Pu}$ is therefore a consequence of mixing
513 between sediment labeled by nuclear effluent releases into the Rhone River and
514 erosion of soil material from the catchment (Eyrolle et al. 2004).

515 The highest contribution of Pu-labeled sediment remobilisation occurred during
516 floods characterised by the highest water discharges (82-88 % for ^{238}Pu and 36-47 %
517 for $^{239+240}\text{Pu}$ on 11/26/2002, 12/02/2003 and 12/03/2003, Table 3). The
518 contribution of remobilised sediment is controlled by specific physical properties of
519 sediment during reworking processes, such as critical shear stress (Lau and Droppo
520 2000; Gerbersdorf et al. 2007), which can be enhanced with increasing water
521 discharge.

522 However, high contributions (> 70 % for ^{238}Pu) of Pu-labeled remobilised sediment
523 were also recorded during intermediate floods, suggesting that water discharge is
524 not the single factor controlling sediment remobilisation. The proportion of Pu
525 derived from the remobilisation of sediment is also controlled by the flush of

526 temporarily stored sediment and the heterogeneous labelling of sediment by Pu
527 (Eyrolle et al. 2012).

528

529 At a given discharge, the fraction of remobilised sediment enriched in Pu displays a
530 large inter- and intra-flood variability, suggesting the lack of control achieved by
531 the suspended sediment origin and the flood type (Table 3). For example, at
532 discharges comprised between 4,000 and 4,100 m³.s⁻¹, the fraction of remobilised
533 sediment varies by a factor of 2 between two Cevenol floods in November 2008 and
534 2011. At ~5,300 m³.s⁻¹, the remobilised sediment fraction varies by a similar factor
535 between generalised and Cevenol floods that occurred in November 2002 and 2008.
536 The fractions of Pu-labeled remobilised sediment reached minimum values during
537 the flood of May 2008 (4-5 % for ²³⁸Pu, Table 3), indicating an unusual supply of Pu-
538 depleted sediment that was attributed to simultaneous dam releases that occurred
539 upstream of Marcoule reprocessing plant and that likely supplied material depleted
540 in plutonium (Eyrolle et al. 2012).

541

542 Although sediment reworking occurs routinely and a substantial decrease of
543 Marcoule plutonium releases was documented after 1997 (Eyrolle et al. 2005), we
544 could not observe any significant decreasing trend in Pu AR evolution between 2000
545 and 2011, suggesting that the stock of Pu-labeled sediment may not have
546 decreased significantly at a decadal timescale or that Pu releases continued
547 significantly after 1997.

548 4.3.2 Activity ratio ¹³⁷Cs/²³⁹⁺²⁴⁰Pu

549 4.3.2.1 In soils

550 The spatial distribution of ¹³⁷Cs/²³⁹⁺²⁴⁰Pu activity ratio in soils estimated based on
551 the theoretical deposition of both radionuclides is heterogeneous across the Rhone
552 River basin (Figure 5).

553 The mean Cs/Pu AR estimated for each subcatchment was systematically higher
554 than the ratio characteristic of global atmospheric fallout (i.e., 27-42), reflecting
555 the additional supply of ¹³⁷Cs from Chernobyl accident (Table 4). In the southern
556 part of the Rhone basin (Figure 5, Table 4), the East-West decreasing gradient of
557 this ratio clearly indicates that soils drained by Pre-Alpine tributaries (Durance,
558 Aigues, Ouveze, Drome rivers) were more contaminated by Chernobyl ¹³⁷Cs fallout

559 (Cs/Pu AR between 108-136) than those drained by Cevenol tributaries (Ardeche,
560 Gard, Ceze river; Cs/Pu AR between 47-56).

561 4.3.2.2 In suspended sediments

562 Activities in ^{137}Cs of suspended sediments varied between 3.0 ± 0.4 and $35\pm 3 \text{ Bq.kg}^{-1}$
563 (Supplementary information Table S5). This variability may reflect the difference in
564 sediment origin, as it was shown that grain size did not significantly influence
565 activities in ^{137}Cs of suspended sediment transported during floods at this station
566 (Antonelli et al. 2008). The mean ^{137}Cs activity for the period 2001-2012 was
567 estimated to $10\pm 5 \text{ Bq.kg}^{-1}$, which is lower although not significantly different from
568 annual records documenting the “anthropogenic background” of the Rhone basin
569 (i.e., $14.9\pm 0.4 \text{ Bq.kg}^{-1}$ reported by Antonelli et al. 2008, and $15\pm 4 \text{ Bq.kg}^{-1}$ reported
570 by Eyrolle et al. 2012).

571
572 Contrary to $^{238}\text{Pu}/^{239+240}\text{Pu}$, a specific $^{137}\text{Cs}/^{239+240}\text{Pu}$ activity ratio could not be
573 attributed to radioactive liquid releases of Marcoule reprocessing plant.
574 Estimations vary between 24 and 3,727, and this range of values is too broad for
575 quantifying the specific contribution of these radioactive releases to suspended
576 sediment.

577
578 When plotting $^{239+240}\text{Pu}$ vs. ^{137}Cs activities in suspended sediment collected during
579 floods, the obtained positive relationship confirms the contribution of a single
580 source (i.e., erosion of Rhone catchment soils) supplying both radionuclides to the
581 lower Rhone River (Figure 6, data are given in Supplementary information Table
582 S5), and that the contribution of $^{239+240}\text{Pu}$ originating from the remobilisation of
583 sediment downstream of Marcoule may be considered to be of minor importance
584 compared to catchment contribution (Table 3).

585
586 Cs/Pu ARs measured in suspended sediment were systematically higher than the
587 characteristic global atmospheric fallout ratio (i.e., 27-42), reflecting the
588 additional input of ^{137}Cs from the Chernobyl fallout (Supplementary information
589 Table S5).

590

591 Although $^{239+240}\text{Pu}$ and ^{137}Cs activities in suspended sediment conveyed during floods
592 are correlated (Figure 6), the mean $^{137}\text{Cs}/^{239+240}\text{Pu}$ activity ratio slightly differed for
593 the different flood types. As expected from the mapping of Cs/Pu AR in the
594 southern part of the Rhone basin, suspended sediment that originated from
595 Cevenol tributaries displayed the mean lowest Cs/Pu AR (i.e., 54 ± 6) whereas
596 suspended sediment supplied by Pre-Alpine tributaries displayed the mean highest
597 Cs/Pu AR (i.e., 78 ± 10). Sediment exported during generalised floods showed a
598 higher variability in Cs/Pu AR due to the mix of the various potential sediment
599 sources at the entire Rhone basin scale (mean Cs/Pu AR equal to 71 ± 16). No
600 specific signature was expected in suspended sediment exported during Oceanic
601 floods (mean Cs/Pu AR equal to 70 ± 17), since Upstream sediment source was
602 characterised by intermediary Cs/Pu AR values comprised between the signatures
603 of Cevenol and Pre-Alpine sediment sources.

604 4.3.3 Expected and calculated Cs/Pu AR in suspended sediment

605 Based on the theoretical value of $^{137}\text{Cs}/^{239+240}\text{Pu}$ activity ratio in soils of the
606 different subcatchments (Table 4), each potential sediment source was
607 characterised by its mean Cs/Pu AR: 132 ± 19 , 73 ± 22 and 51 ± 5 for Pre-Alpine,
608 Upstream and Cevenol sources, respectively. By combining artificial radionuclide
609 characteristics for these three sediment sources and the contribution of each
610 sediment source (in percentage) obtained by the fingerprinting method based on
611 natural radionuclides (see 3.2.2), the expected Cs/Pu AR were estimated in
612 suspended sediment (Supplementary information Table S5).

613 All Cs/Pu AR calculated from artificial radionuclide measurements conducted on
614 suspended sediment (Cs/Pu AR SS) were comprised in the range of variation of
615 expected Cs/Pu AR (Cs/Pu AR exp). Although values were not significantly
616 different, the discrepancy between expected and calculated Cs/Pu AR generally
617 indicated an underestimation of expected values. This observation may be due to
618 the strong dilution of the initial signature of Cs/Pu AR in soils because of the
619 occurrence of physical and dynamical processes such as erosion, deposition and
620 reworking processes during the decades that followed the last ^{137}Cs inputs in 1986.
621 Alternatively, this underestimation could be due to contribution of sediment
622 depleted in artificial radionuclides and supplied by subsurface erosion such as
623 riverbanks or deep gullies (Ben Slimane et al. 2013; Evrard et al. 2013).

624 **5 Conclusions**

1 625 This study provided to our knowledge the first attempt to combine the use of a
2
3 626 continuous river monitoring network and sediment fingerprinting based on natural
4
5 627 and artificial radionuclides to quantify the respective contribution of
6
7 628 subcatchments to sediment transported during floods at the outlet of a large river
8
9 629 basin (98,000 km²).

10 630

11
12 631 A first fingerprinting method based on measurements of natural radionuclides (²³⁸U,
13
14 632 ²³²Th and ⁴⁰K) allowed the quantification of the relative contribution of each
15
16 633 potential sediment source. The total amount of suspended sediment exported
17
18 634 during floods for the period 2000-2012 was estimated to 19.5x10⁶ tons. Pre-Alpine,
19
20 635 Upstream, and Cevenol sources contributed to 53, 35 and 11 % of the total
21
22 636 sediment supply, respectively. Pre-Alpine tributaries were thereby shown to be
23
24 637 the main sediment supplier to the lower Rhone River during floods. Then, the
25
26 638 results provided by an alternative method based on artificial radionuclide
27
28 639 measurements (¹³⁷Cs/²³⁹⁺²⁴⁰Pu activity ratio) failed to achieve this objective at the
29
30 640 basin scale, because of the heterogeneous spatial pattern of ¹³⁷Cs deposition after
31
32 641 Chernobyl accident that did not coincide with the delineation of the above-
33
34 642 mentioned subcatchment sources. However, it provided a relevant discrimination
35
36 643 between the respective contributions of western and eastern tributaries in the
37
38 644 southern part of the Rhone basin.

39
40 645 In addition, the method based on ²³⁸Pu/²³⁹⁺²⁴⁰Pu activity ratio demonstrated the
41
42 646 continuous remobilisation of local Pu-labeled sediment and showed that the stock
43
44 647 of Pu-contaminated sediment in the Lower Rhone River may not have decreased
45
46 648 significantly during the decade that followed the dismantlement of the spent fuel
47
48 649 reprocessing plant. These natural and artificial radionuclide activities may then
49
50 650 further be used to better understand the fate of sediment supplied to the
51
52 651 Mediterranean Sea.

53 652

54
55 653 In future, fingerprinting based on natural radionuclides could usefully be applied to
56
57 654 catchments characterized by lithological variations. Furthermore, methods based
58
59 655 on artificial radionuclides measurements (¹³⁷Cs/²³⁹⁺²⁴⁰Pu activity ratio) may be
60
61 656 applied to catchments characterised by spatial heterogeneous patterns of ¹³⁷Cs
62
63 657 deposition.
64
65

658 **Acknowledgements**

1 659 This work was supported by the Rhone Sediment Observatory (OSR) from ZABR and
2
3 660 by AERMC (Agence de l'Eau Rhône-Méditerranée-Corse). Liquid discharge data in
4
5 661 the Rhone River and its tributaries were available from the CNR (Compagnie
6
7 662 Nationale du Rhône, <http://www.cnr.tm.fr/fr/>). Daily suspended sediment load
8
9 663 data were provided by Patrick Raimbault (MIO) from MOOSE/SOERE.

10 664 The authors gratefully acknowledge Vincent Boullier, Benoît Rolland and
11
12 665 IRSN/LERCM team, Marc Desmet (GEHCO), Jean Philippe Bedell (ENTPE), and Michel
13
14 666 Fornier (MIO) for their help during field and laboratory works, and IRSN/LMRE team
15
16 667 and Irène Lefèvre (LSCE) for sample analyses.

17
18 668 The authors also gratefully thank the five anonymous reviewers whose suggestions
19
20 669 greatly improved the quality of the manuscript.

21
22 670 **Appendix A. Supplementary data**

23
24 671 Supplementary data associated with this article can be found in the online version.

25
26 672

27
28 673 **References**

- 29 674 Antonelli, C., 2002. Flux sédimentaires et morphogenèse récente dans le
30
31 675 chenal du Rhône aval. Ph.D. thesis, University of Aix-Marseille I., France, 272
32 676 pp.
- 33 677 Antonelli, C., F. Eyrolle, B. Rolland, M. Provansal and F. Sabatier (2008).
34
35 678 "Suspended sediment and ¹³⁷Cs fluxes during the exceptional December 2003
36 679 flood in the Rhone River, southeast France." *Geomorphology* **95**(3-4): 350-
37 680 360.
- 38 681 Antovic, N. M., P. Vukotic, N. Svrkota, S. K. Andrukhovich (2012). "Pu-239+240 and
39 682 Cs-137 in Montenegro soil: their correlation and origin." *Journal of*
40
41 683 *Environmental Radioactivity* **110**: 90-97.
- 42 684 Ben Slimane, A., D. Raclot, O. Evrard, M. Sanaa, I. Lefèvre, M. Ahmadi, M. Tounsi,
43 685 C. Rumpel, A. Ben Mammou, Y. Le Bissonnais (2013). "Fingerprinting
44 686 sediment sources in the outlet reservoir of a hilly cultivated catchment of
45 687 Tunisia." *Journal of Soils and Sediments* **13**(4): 801-815.
- 47 688 Bosc, E., A. Bricaud and D. Antoine (2004). "Seasonal and interannual variability in
48 689 algal biomass and primary production in the Mediterranean Sea, as derived
49 690 from 4 years of SeaWiFS observations." *Global Biogeochemical Cycles* **18**(1):
50 691 GB1005.
- 52 692 Charmasson, S., O. Radakovitch, M. Arnaud, P. Bouisset, A.-S. Pruchon (1998).
53 693 "Long-core profiles of ¹³⁷Cs, ¹³⁴Cs, ⁶⁰Co and ²¹⁰Pb in sediment near the Rhône
54 694 River (Northwestern Mediterranean Sea)." *Estuaries* **21**(3): 367-378.
- 56 695 Cochran, J. K., S. B. Moran, N. S. Fisher, T. M. Beasley and J. M. Kelley (2000).
57 696 "Sources and transport of anthropogenic radionuclides in the Ob River
58 697 system, Siberia." *Earth and Planetary Science Letters* **179**(1): 125-137.

59
60
61
62
63
64
65

- 698 Collins, A. L. and D. E. Walling (2002). "Selecting fingerprint properties for
1 699 discriminating potential suspended sediment sources in river basins." Journal
2 700 of Hydrology **261**(1-4): 218-244.
- 3 701 Delmas, M., O. Cerdan, B. Cheviron, J.-M. Mouchel, F. Eyrolle (2012). "Sediment
4 702 export from French rivers to the sea." Earth Surface Processes and
5 703 Landforms **37**(7): 754-762.
- 6 704 Desmet, M., B. Mourier, B. J. Mahler, P. C. Van Metre, G. Roux, H. Persat, I.
7 705 Lefèvre, A. Peretti, E. Chapron, A. Simonneau, C. Miège and M. Babut
8 706 (2012). "Spatial and temporal trends in PCBs in sediment along the lower
9 707 Rhône River, France." Science of the Total Environment **433**(0): 189-197.
- 10 708 Dufois, F., R. Verney, P. Le Hir, F. Dumas and S. Charmasson (2014) "Impact of
11 709 winter storms on sediment erosion in the Rhone River prodelta and fate of
12 710 sediment in the Gulf of Lions (North Western Mediterranean Sea)."
13 711 Continental Shelf Research **72**: 57-72.
- 14 712 Durrieu de Madron, X., C. Guieu, R. Sempéré, P. Conan, D. Cossa, F. D'Ortenzio, C.
15 713 Estournel, F. Gazeau, C. Rabouille, L. Stemmann, S. Bonnet, F. Diaz, P.
16 714 Koubbi, O. Radakovitch, M. Babin, M. Baklouti, C. Bancon-Montigny, S.
17 715 Belviso, N. Bensoussan, B. Bonsang, I. Bouloubassi, C. Brunet, J. F. Cadiou,
18 716 F. Carlotti, M. Chami, S. Charmasson, B. Charrière, J. Dachs, D. Doxaran, J.
19 717 C. Dutay, F. Elbaz-Poulichet, M. Eléaume, F. Eyrolles, C. Fernandez, S.
20 718 Fowler, P. Francour, J. C. Gaertner, R. Galzin, S. Gasparini, J. F. Ghiglione,
21 719 J. L. Gonzalez, C. Goyet, L. Guidi, K. Guizien, L. E. Heimbürger, S. H. M.
22 720 Jacquet, W. H. Jeffrey, F. Joux, P. Le Hir, K. Leblanc, D. Lefèvre, C.
23 721 Lejeusne, R. Lemé, M. D. Loÿe-Pilot, M. Mallet, L. Méjanelle, F. Mélin, C.
24 722 Mellon, B. Mérigot, P. L. Merle, C. Migon, W. L. Miller, L. Mortier, B.
25 723 Mostajir, L. Mousseau, T. Moutin, J. Para, T. Pérez, A. Petrenko, J. C.
26 724 Poggiale, L. Prieur, M. Pujo-Pay, V. Pulido, P. Raimbault, A. P. Rees, C.
27 725 Ridame, J. F. Rontani, D. Ruiz Pino, M. A. Sicre, V. Taillandier, C.
28 726 Tamburini, T. Tanaka, I. Taupier-Letage, M. Tedetti, P. Testor, H. Thébault,
29 727 B. Thouvenin, F. Touratier, J. Tronczynski, C. Ulses, F. Van Wambeke, V.
30 728 Vantrepotte, S. Vaz and R. Verney (2011). "Marine ecosystems' responses to
31 729 climatic and anthropogenic forcings in the Mediterranean." Progress in
32 730 Oceanography **91**(2): 97-166.
- 33 731 Evrard, O., O. Navratil, S. Ayrault, M. Ahmadi, J. Némery, C. Legout, I. Lefèvre, A.
34 732 Poirel, P. Bonté and M. Esteves (2011). "Combining suspended sediment
35 733 monitoring and fingerprinting to determine the spatial origin of fine
36 734 sediment in a mountainous river catchment." Earth Surface Processes and
37 735 Landforms **36**(8): 1072-1089.
- 38 736 Evrard, O., J. Poulénard, J. Némery, S. Ayrault, N. Gratiot, C. Duvert, C. Prat, I.
39 737 Lefèvre, P. Bonté, M. Esteves (2013). "Tracing sediment sources in a tropical
40 738 highland catchment of central Mexico by using conventional and alternative
41 739 fingerprinting methods." Hydrological Processes **27**: 911-922.
- 42 740 Eyrolle, F., S. Charmasson, D. Louvat (2004). "Plutonium isotopes in the lower
43 741 reaches of the River Rhône over the period 1945-2000: fluxes towards the
44 742 Mediterranean Sea and sedimentary inventories." Journal of Environmental
45 743 Radioactivity **74**: 127-138.
- 46 744 Eyrolle, F., D. Louvat, J.-M. Métivier, B. Rolland (2005). "Origins and levels of
47 745 artificial radionuclides within the Rhône river waters (France) for the last
48 746 forty years: Towards an evaluation of the radioecological sensitivity of river
49 747 systems." Radioprotection **40**(4): 435-446.
- 50
51
52
53
54
55
56
57
58
59
60
61
62
63
64
65

- 748 Eyrolle, F., C. Duffa, C. Antonelli, B. Rolland and F. Leprieur (2006). "Radiological
1 749 consequences of the extreme flooding on the lower course of the Rhone
2 750 valley (December 2003, South East France)." Science of the Total
3 751 Environment **366**(2-3): 427-438.
- 4 752 Eyrolle, F., Claval D., Gontier G. and Antonelli C. (2008). "Radioactivity level in
5 753 major French rivers: summary of monitoring chronicles acquired over the
6 754 past thirty years and current status." Journal of Environmental Monitoring
7 755 **10**: 800-811.
- 8 756 Eyrolle, F., O. Radakovitch, P. Raimbault, S. Charmasson, C. Antonelli, E. Ferrand,
9 757 D. Aubert, G. Raccasi, S. Jacquet and R. Gurriaran (2012). "Consequences of
10 758 hydrological events on the delivery of suspended sediment and associated
11 759 radionuclides from the Rhône River to the Mediterranean Sea." Journal of
12 760 Soils and Sediments **12**(9): 1479-1495.
- 13 761 Ferrand, E., F. Eyrolle, O. Radakovitch, M. Provansal, S. Dufour, C. Vella, G.
14 762 Raccasi and R. Gurriaran (2012). "Historical levels of heavy metals and
15 763 artificial radionuclides reconstructed from overbank sediment records in
16 764 lower Rhône River (South-East France)." Geochimica et Cosmochimica Acta
17 765 **82**: 163-182.
- 18 766 Fohrer, N., and L. Chicharo (2011). "Interaction of River Basins and Coastal Waters-
19 767 An Integrated Ecohydrological View" Reference Module in Earth Systems and
20 768 Environmental Sciences - Treatise on Estuarine and Coastal Science **10**: 109-
21 769 150.
- 22 770 Garcia-Orellana, J., J.M. Pates, P. Masqué, J.M. Bruach, J.A. Sanchez-Cabeza,
23 771 (2009). "Distribution of artificial radionuclides in deep sediments of the
24 772 Mediterranean Sea." Science of the Total Environment **407**(2):887-898.
- 25 773 Gerbersdorf, S. U., T. Jancke and B. Westrich (2007). "Sediment properties for
26 774 assessing the erosion risk of contaminated riverine sites. A comprehensive
27 775 approach to evaluate sediment properties and their covariance patterns over
28 776 depth in relation to erosion resistance - First investigations in natural
29 777 sediments at three contaminated reservoirs." Journal of Soils and Sediments
30 778 **7**(1): 25-35.
- 31 779 Goutelard, F., M. Morello and D. Calmet (1998). "Alpha-spectrometry measurement
32 780 of Am and Cm at trace levels in environmental samples using extraction
33 781 chromatography." Journal of Alloys and Compounds **271-273**: 25-30.
- 34 782 Haddadchi, A., D. S. Ryder, O. Evrard, J. Olley (2013). "Sediment fingerprinting in
35 783 fluvial systems: Review of tracers, sediment sources and mixing models."
36 784 International Journal of Sediment Research **28**(4): 560-578.
- 37 785 Hodge, V., C. Smith and J. Whiting (1996). "Radiocaesium and Plutonium: Still
38 786 together in "background" soils." Chemosphere **32**(10): 2067-2075.
- 39 787 Lansard, B., S. Charmasson, C. Gascó, M. P. Antón, C. Grenz and M. Arnaud (2007).
40 788 "Spatial and temporal variations of plutonium isotopes (^{238}Pu and $^{239,240}\text{Pu}$) in
41 789 sediments off the Rhone River mouth (NW Mediterranean)." Science of the
42 790 Total Environment **376**(1-3): 215-227.
- 43 791 Lau, Y. L. and I. G. Droppo (2000). "Influence of antecedent conditions on critical
44 792 shear stress of bed sediments." Water Research **34**(2): 663-667.
- 45 793 Le Cloarec, M.-F., P. Bonté, I. Lefèvre, J.-M. Mouchel, and S. Colbert (2007).
46 794 "Distribution of ^7Be , ^{210}Pb and ^{137}Cs in watersheds of different scales in the
47 795 Seine River basin: Inventories and residence times." Science of the Total
48 796 Environment **375**: 125-139.

- 797 Lee, S.-H., J.J. La Rosa, I. Levy-Palomo, B. Oregioni, M. K. Pham, P. P. Povinec, E.
1 798 Wyse (2003). "Recent inputs and budgets of ^{90}Sr , ^{137}Cs , $^{239,240}\text{Pu}$ and ^{241}Am in
2 799 the northwest Mediterranean Sea." Deep Sea Research Part II: Topical
3 800 Studies in Oceanography **50**(17-21): 2817-2834.
- 4 801 Le Roux, G., C. Duffa, F. Vray and P. Renaud (2010). "Deposition of artificial
5 802 radionuclides from atmospheric Nuclear Weapon Tests estimated by soil
6 803 inventories in French areas low-impacted by Chernobyl." Journal of
7 804 Environmental Radioactivity **101**(3): 211-218.
- 8 805 Lefèvre, O., P. Bouisset, P. Germain, E. Barker, G. Kerlau and X. Cagnat (2003).
9 806 "Self-absorption correction factor applied to ^{129}I measurement by direct
10 807 gamma-X spectrometry for *Fucus serratus* samples." Nuclear Instruments and
11 808 Methods in Physics Research, Section A: Accelerators, Spectrometers,
12 809 Detectors and Associated Equipment **506**(1-2): 173-185.
- 13 810 Ludwig, W., E. Dumont, M. Meybeck and S. Heussner (2009). "River discharges of
14 811 water and nutrients to the Mediterranean and Black Sea: Major drivers for
15 812 ecosystem changes during past and future decades?" Progress in
16 813 Oceanography **80**(3-4): 199-217.
- 17 814 Masson, O., D. Piga, R. Gurriaran, and D. D'Amico (2010). " Impact of an
18 815 exceptional Saharan dust outbreak in France: PM10 and artificial
19 816 radionuclides concentrations in air and in dust deposit." Atmospheric
20 817 Environment **44**: 2478-2486.
- 21 818 Motha, J.A., P.J. Wallbrink, P.B. Hairsine, R.B. Grayson (2003). "Determining the
22 819 sources of suspended sediment in a forested catchment in southeastern
23 820 Australia." Water Resources Research **39**: 1059.
- 24 821 Meybeck, M., H. H. Dürr, S. Roussennac and W. Ludwig (2007). "Regional seas and
25 822 their interception of riverine fluxes to oceans." Marine Chemistry **106**(1-2):
26 823 301-325.
- 27 824 Meybeck, M., L. Laroche, H. H. Dürr and J. P. M. Syvitski (2003). "Global variability
28 825 of daily total suspended solids and their fluxes in rivers." Global and
29 826 Planetary Change **39**(1-2): 65-93.
- 30 827 Meybeck, M. and C. Vörösmarty (2005). "Fluvial filtering of land-to-ocean fluxes:
31 828 from natural Holocene variations to Anthropocene." Comptes Rendus
32 829 Geoscience **337**(1-2): 107-123.
- 33 830 Miralles, J., O. Radakovitch, J. K. Cochran, A. Véron and P. Masqué (2004).
34 831 "Multitracer study of anthropogenic contamination records in the Camargue,
35 832 Southern France." Science of the Total Environment **320**(1): 63-72.
- 36 833 Mitchell, P., J. Sanchez-Cabeza, T. Ryan, A. McGarry, A. Vidal-Quatras (1990).
37 834 "Preliminary estimates of cumulative caesium and plutonium deposition in
38 835 the Irish terrestrial environment." Journal of Radioanalytical and nuclear
39 836 Chemistry **138**(2): 241-256.
- 40 837 Mourier, B., M. Desmet, P.C. Van Metre, B.J. Mahler, Y. Perrodin, G. Roux, J.-P.
41 838 Bedell, I. Lefèvre, M. Babut (2014). "Historical records, sources, and spatial
42 839 trends of PCBs along the Rhône River (France)." Science of the Total
43 840 Environment **476-477**: 568-576.
- 44 841 Navratil, O., O. Evrard, M. Esteves, S. Ayrault, I. Lefèvre, C. Legout, J.-L. Reyss, N.
45 842 Gratiot, J. Némery, N. Mathys, A. Poirel and P. Bonté (2012). "Core-derived
46 843 historical records of suspended sediment origin in a mesoscale mountainous
47 844 catchment: the River Bleone, French Alps." Journal of Soils and
48 845 Sediments **12**(9): 1463-1478.
- 49
50
51
52
53
54
55
56
57
58
59
60
61
62
63
64
65

- 846 Olley, J. M., A. S. Murray, D. H. Mackenzie and K. Edwards (1993). "Identifying
1 847 sediment sources in a gullied catchment using natural and anthropogenic
2 848 radioactivity." Water Resources Research **29**(4): 1037-1043.
- 3 849 Ollivier, P., B. Hamelin and O. Radakovitch (2010). "Seasonal variations of physical
4 850 and chemical erosion: A three-year survey of the Rhone River (France)."
5 851 Geochimica et Cosmochimica Acta **74**(3): 907-927.
- 6 852 Ollivier, P., O. Radakovitch and B. Hamelin (2011). "Major and trace element
7 853 partition and fluxes in the Rhône River." Chemical Geology **285**(1-4): 15-31.
- 8 854 Pont, D., J. P. Simonnet and A. V. Walter (2002). "Medium-term changes in
9 855 suspended sediment delivery to the ocean: Consequences of catchment
10 856 heterogeneity and river management (Rhône River, France)." Estuarine,
11 857 Coastal and Shelf Science **54**(1): 1-18.
- 12 858 Radakovitch, O., V. Roussiez, P. Ollivier, W. Ludwig, C. Grenz and J.-L. Probst (2008).
13 859 "Input of particulate heavy metals from rivers and associated sedimentary
14 860 deposits on the Gulf of Lion continental shelf." Estuarine, Coastal and Shelf
15 861 Science **77**(2): 285-295.
- 16 862 Raimbault, P. and X. Durrieu de Madron (2003). "Research activities in the Gulf of
17 863 Lion (NW Mediterranean) within the 1997-2001 PNEC project." Oceanologica
18 864 Acta **26**(4): 291-298.
- 19 865 Renaud, P., L. Pourcelot, J. M. Métivier and M. Morello (2003). "Mapping of ¹³⁷Cs
20 866 deposition over eastern France 16 years after the Chernobyl accident."
21 867 Science of the Total Environment **309**(1-3): 257-264.
- 22 868 Renaud, P., D. Champion, J. Brenot (2007). "Les retombées radioactives de
23 869 l'accident de Tchernobyl sur le territoire français : Conséquences
24 870 environnementales et exposition des personnes." Editions Tec&Doc,
25 871 Lavoisier, 208 pp.
- 26 872 Rolland, B., 2006. Transfert des radionucléides artificiels par voie fluviale:
27 873 conséquences sur les stocks sédimentaires rhodaniens et les exports vers la
28 874 Méditerranée. Ph.D. thesis, University of Paul Cezanne Aix-Marseille, France,
29 875 322 pp.
- 30 876 Roussel-Debel, S., P. Renaud and J. M. Métivier (2007). "¹³⁷Cs in French soils:
31 877 Deposition patterns and 15-year evolution." Science of the Total
32 878 Environment **374**(2-3): 388-398.
- 33 879 Sempéré, R., B. Charrière, F. Van Wambeke and G. Cauwet (2000). "Carbon inputs
34 880 of the Rhône River to the Mediterranean Sea: Biogeochemical implications."
35 881 Global Biogeochemical Cycles **14**(2): 669-681.
- 36 882 Sicre, M. A., M. B. Fernandes and D. Pont (2008). "Poly-aromatic hydrocarbon (PAH)
37 883 inputs from the Rhône River to the Mediterranean Sea in relation with the
38 884 hydrological cycle: Impact of floods." Marine Pollution Bulletin **56**: 1935-
39 885 1942.
- 40 886 Syvitski, J. P. M. and A. J. Kettner (2007). "On the flux of water and sediment into
41 887 the Northern Adriatic Sea." Continental Shelf Research **27**(3-4): 296-308.
- 42 888 Syvitski, J. P. M., C. J. Vörösmarty, A. J. Kettner and P. Green (2005). "Impact of
43 889 Humans on the Flux of Terrestrial Sediment to the Global Coastal Ocean."
44 890 Science **308**(5720): 376-380.
- 45 891 Thomas, A. J. (1997). "Input of artificial radionuclides to the Gulf of Lions and
46 892 tracing the Rhone influence in marine surface sediments." Deep-Sea
47 893 Research Part II: Topical Studies in Oceanography **44**(3-4): 577-595.
- 48 894 Turner, M., M. Rudin, J. Cizdziel and V. Hodge (2003). "Excess plutonium in soil
49 895 near the Nevada Test Site, USA." Environmental Pollution **125**: 193-203.
- 50
51
52
53
54
55
56
57
58
59
60
61
62
63
64
65

- 896 Walling, D. E. and A. L. Collins (2008). "The catchment sediment budget as a
1 897 management tool." Environmental Science & Policy **11**(2): 136-143.
- 2 898 Yeager, K. M. and P. H. Santschi (2003). "Invariance of isotope ratios of lithogenic
3 899 radionuclides: more evidence for their use as sediment source tracers."
4 900 Journal of Environmental Radioactivity **69**(3): 159-176.
- 5 901 Zebracki, M., F. Eyrolle-Boyer, A. De Vismes-Ott, C. Antonelli, X. Cagnat and V.
6 902 Boullier (2013a). "Radionuclide Contents in Suspended Sediments in Relation
7 903 to Flood Types in the Lower Rhone River." Procedia Earth and Planetary
8 904 Science **7**: 936-939.
- 9 905 Zebracki, M., F. Eyrolle, X. Cagnat, C. Antonelli, A. De Vismes-Ott and V. Boullier
10 906 (2013b). "Characterisation of naturally occurring radionuclides in the lower
11 907 Rhone River (France): Preliminary results from suspended solid monitoring."
12 908 WIT Transactions on Ecology and the Environment **171**: 235-245.
- 13 909
14 910
15 911
16 912
17 913
18 914
19 915
20 916
21 917
22 918
23 919
24 920
25 921
26 922
27 923
28 924
29 925
30 926
31 927
32 928
33 929
34 930
35 931
36 932
37 933
38 934
39 935
40 936
41 937
42 938
43 939
44 940
45 941
46 942
47 943
48 944
49 945
50 946
51 947
52 948
53 949
54 950
55 951
56 952
57 953
58 954
59 955
60 956
61 957
62 958
63 959
64 960
65 961

Figure caption

Figure 1 : Map of the Rhone River catchment. Location of the river monitoring sampling station at Arles and sampling sites of sediment representative of each subcatchment source is indicated. Boundaries of subcatchment areas where the different flood types are generated are also indicated: Oceanic, Cevenol, extensive Mediterranean, and Generalised.

Figure 2 : Boxplot of activities in ^{238}U , ^{232}Th and ^{40}K , in Bq.kg^{-1} , in suspended sediment collected in the Lower Rhone River according the four flood types: 1 Oceanic, 2 Cevenol, 3 Extensive Mediterranean, 4 Generalised.

Figure 3 : Boxplot of sediment supply contribution (%) of each sediment source during (a) Oceanic, (b) Cevenol, (c) extensive Mediterranean and (d) generalised floods.

Figure 4 : Suspended sediment load (in 10^6 ton) discharged during floods in the Lower Rhone River between 2001 and 2011 according to the sediment source (a) and the flood type (b).

Figure 5 : Theoretical activity ratio in $^{137}\text{Cs}/^{239+240}\text{Pu}$ across the Rhone River basin (values decay-corrected to 1/1/2010).

Figure 6 : Plot of $^{239+240}\text{Pu}$ vs. ^{137}Cs activities, in Bq.kg^{-1} of dry matter, in suspended sediment collected in the Lower Rhone River during floods.

Figure 1
Click here to download Figure: Figure 1 revised.pdf

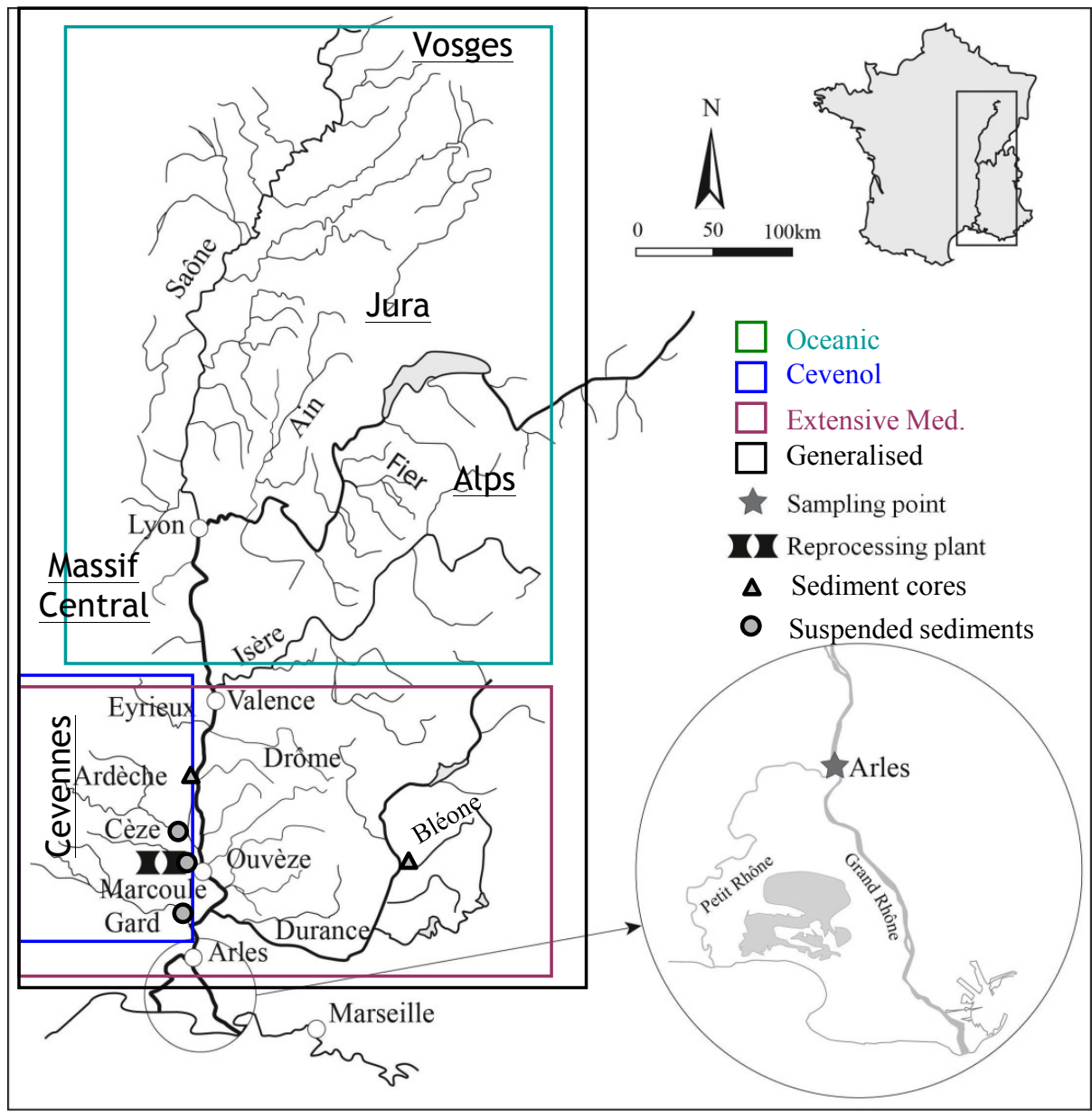
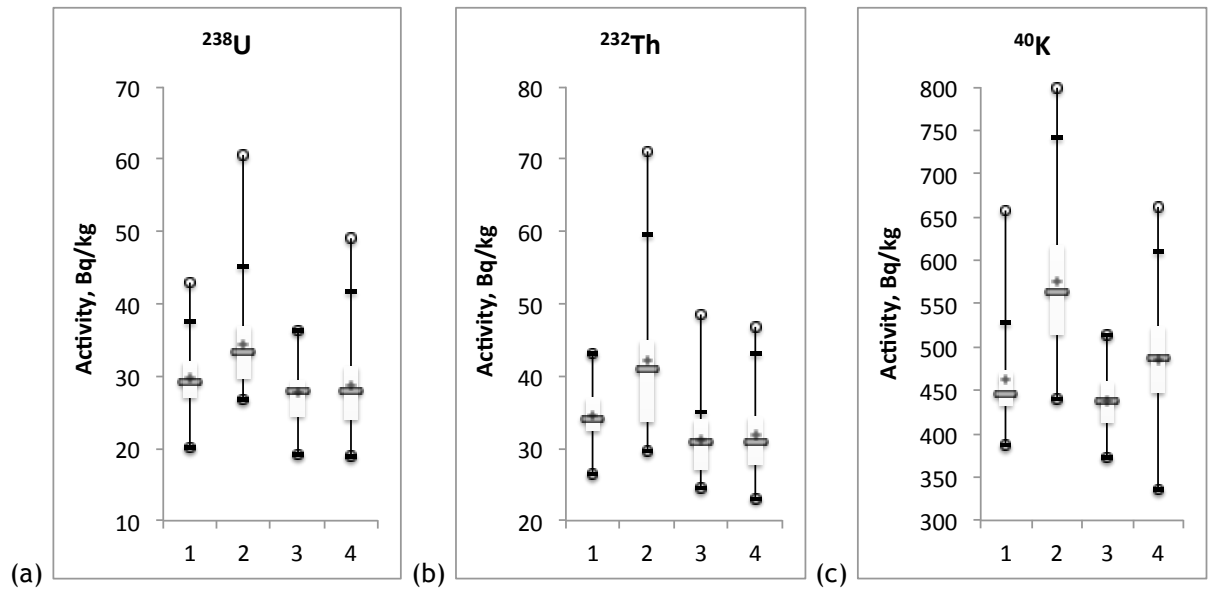
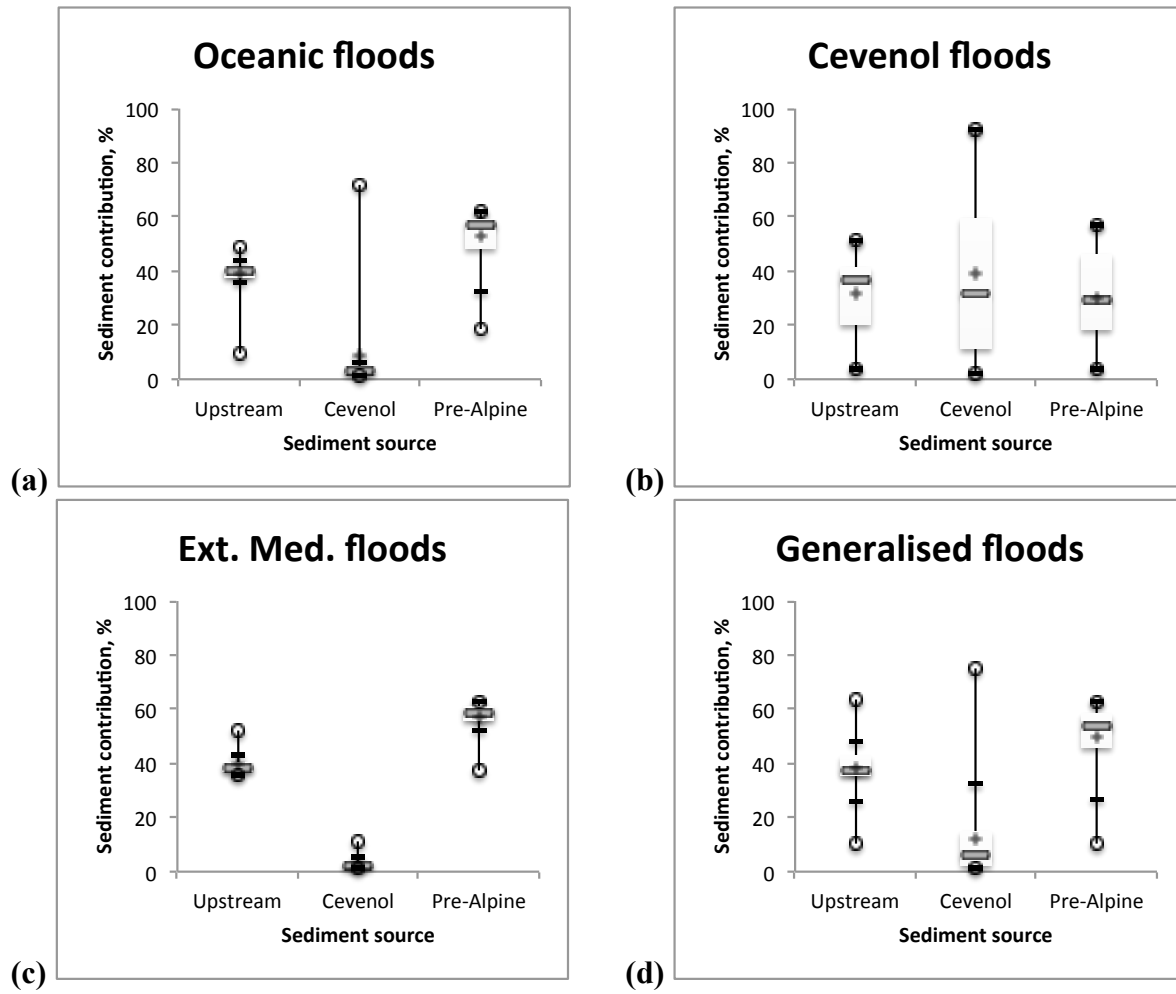


Figure 2
[Click here to download Figure: Figure 2 revised.pdf](#)





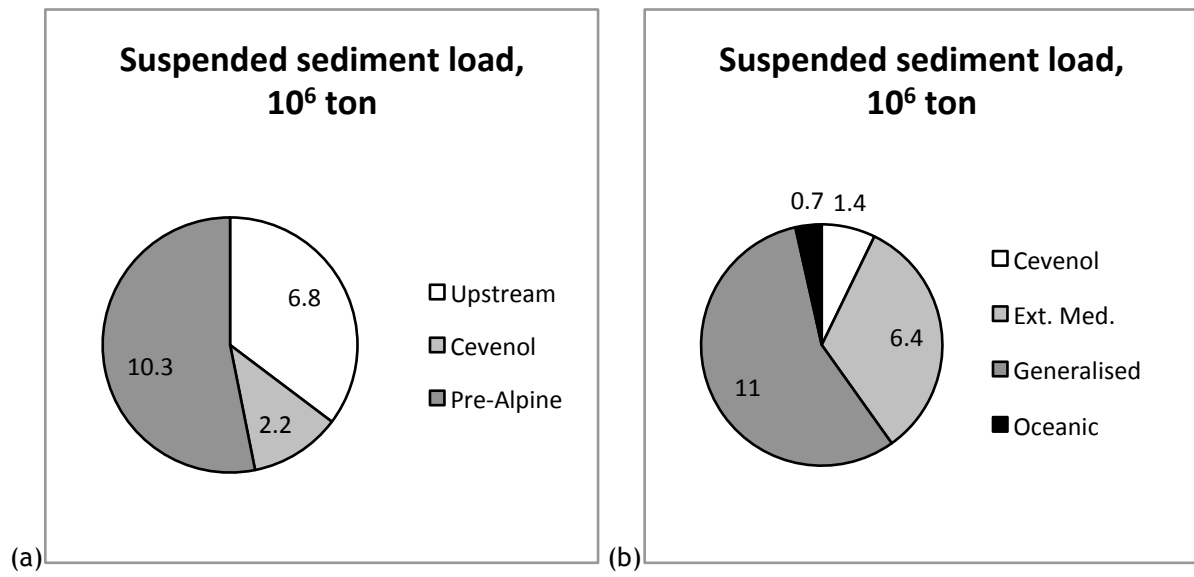


Figure 5
[Click here to download Figure: Figure 5 revised.pdf](#)

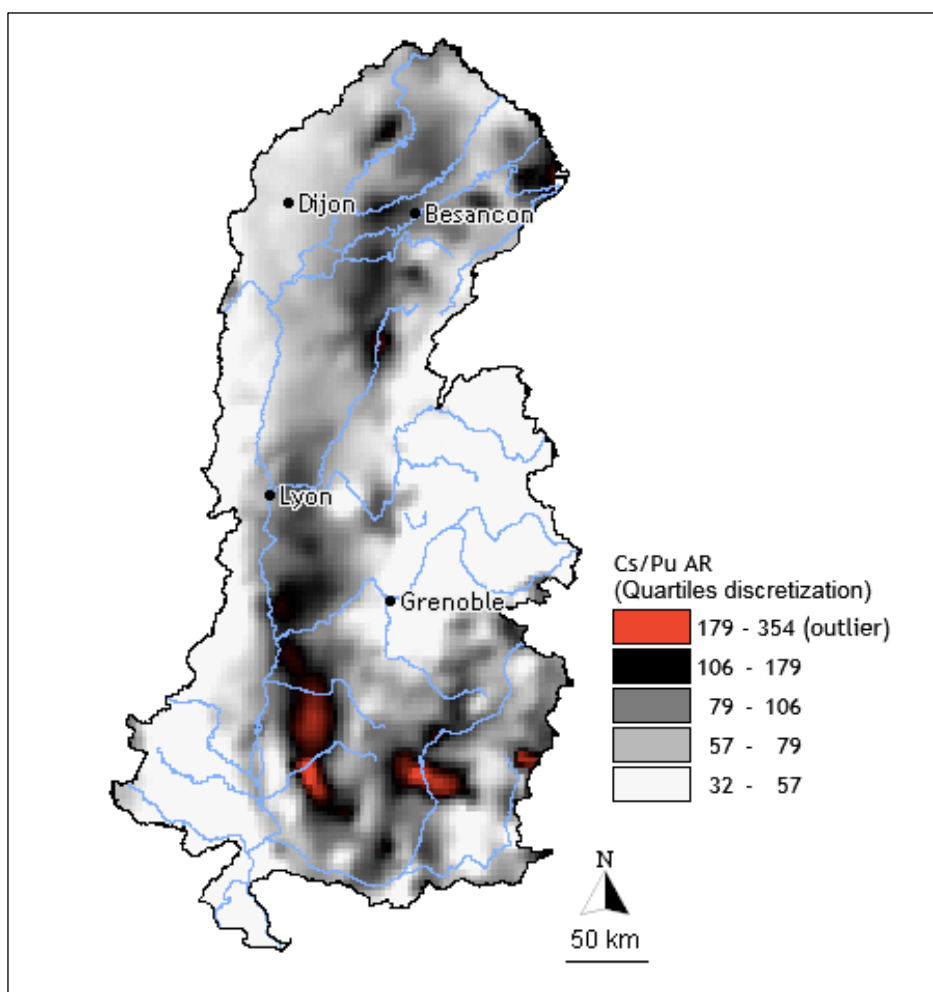


Figure 6
[Click here to download Figure: Figure 6.pdf](#)

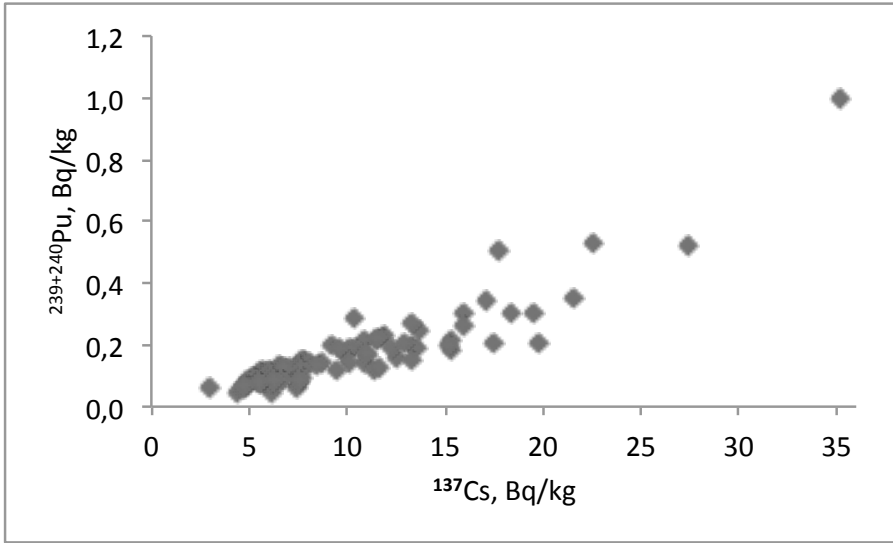


Table caption

[Click here to download Table: Table caption revised.pdf](#)

Table 1 : List of investigated flood events, number of collected samples, occurrence of different flood types: Oceanic, Mediterranean, extensive Mediterranean and [generalised](#). The maximum hourly (*daily) water discharge value for each flood event is mentioned between brackets.

[Table 2 : Mean radionuclide activities, in Bq.kg⁻¹ dry weight, measured in representative sediment source samples collected in each subcatchment.](#)

Table 3 : Activities in ²³⁸Pu and ²³⁹⁺²⁴⁰Pu, ²³⁸Pu/²³⁹⁺²⁴⁰Pu activity ratio (Pu AR) and Pu isotopes fractions originating from sediment remobilisation downstream of Marcoule, of suspended sediment collected during floods at water discharge [exceeding 4,000 m³.s⁻¹ \(when direct radioactive releases were forbidden\)](#).

Table 4 : Theoretical ¹³⁷Cs/²³⁹⁺²⁴⁰Pu activity ratio in soils of Rhone River subcatchments.

Table 1[Click here to download Table: Table 1 revised.pdf](#)

Flood type	Number of flood events	Number of samples	Flood occurrences (maximum water discharge, in $\text{m}^3 \cdot \text{s}^{-1}$)
Oceanic	11	51	2001: Mar(5828*), Apr(3401*); 2004: Jan(3900); 2005: Apr(3726); 2006: Mar(2978), Apr(3940,3922); 2007: Mar(3452); 2008: Apr(3473), Sep(3134); 2010: Jun(3122); 2012: Jan(3924)
Cevenol	8	50	2002: Sep(9019), 2006: Oct(3225), Nov(4529); 2008: Oct(4178), Nov(5621); 2009: Feb(4046); 2010: May(3540); 2011: Nov(4057)
Extensive Mediterranean	4	25	2003: Dec(9757); 2008: Jan(3318), Apr(3449), Dec(4128)
Generalised	12	89	2000: Nov(3888*); 2002: Nov(9100); 2003: Nov(3577); 2004: Oct(4400); 2006: Dec(3533); 2007: Nov(3302); 2008: May(4310); 2009: Feb(4046), Dec(4401); 2010: Feb(3485), Mar(3670), Dec(3907)
Not defined	2	6	2010: Mar(3012), Sep(2190)

Table 2

[Click here to download Table: Table 2 revised.pdf](#)

Sediment source		²³⁸ U	²³² Th	⁴⁰ K
Upstream	Number of samples	12	12	12
	Mean activity, Bq.kg ⁻¹	36	37	512
	<i>sd(1σ)</i>	6	4	39
Pre-Alpine	Number of samples	21	21	21
	Mean activity, Bq.kg ⁻¹	25	30	486
	<i>sd(1σ)</i>	4	3	66
Cevenol	Number of samples	11	11	11
	Mean activity, Bq.kg ⁻¹	47	56	674
	<i>sd(1σ)</i>	12	15	87

Table 3

[Click here to download Table: Table 3.pdf](#)

Sampling time		Flood type	Discharge $\text{m}^3 \cdot \text{s}^{-1}$	^{238}Pu $\text{Bq} \cdot \text{kg}^{-1}$ dry	\pm <i>0,0020</i>	$^{239+240}\text{Pu}$ $\text{Bq} \cdot \text{kg}^{-1}$ dry	\pm <i>0,012</i>	PuAr	\pm <i>0,014</i>	$^{238}\text{Pu}_{\text{Sed}}$ %	$^{239+240}\text{Pu}_{\text{Sed}}$ %
9/10/2002	11:20		7822	0,0138	<i>0,0020</i>	0,200	<i>0,012</i>	0,069	<i>0,014</i>	54	12
9/10/2002	12:25	Cevenol	7189	0,0112	<i>0,0017</i>	0,190	<i>0,011</i>	0,059	<i>0,013</i>	44	9
9/10/2002	13:30		6493	0,0102	<i>0,0016</i>	0,168	<i>0,010</i>	0,061	<i>0,013</i>	46	9
11/19/2002	15:25		7135	0,0305	<i>0,0132</i>	0,306	<i>0,025</i>	0,099	<i>0,051</i>	72	24
11/23/2002	12:15	Generalised	5313	0,0097	<i>0,0050</i>	0,208	<i>0,013</i>	0,047	<i>0,027</i>	26	4
11/26/2002	15:55		9172	0,0339	<i>0,0087</i>	0,261	<i>0,022</i>	0,130	<i>0,044</i>	82	36
12/2/2003	16:40		8060	0,0318	<i>0,0037</i>	0,203	<i>0,011</i>	0,157	<i>0,027</i>	88	46
12/3/2003	11:05	Extensive	10304	0,0488	<i>0,0056</i>	0,303	<i>0,017</i>	0,161	<i>0,028</i>	88	47
12/4/2003	14:00	Mediterranean	9164	0,0216	<i>0,0029</i>	0,200	<i>0,011</i>	0,108	<i>0,021</i>	76	27
12/5/2003	16:25		4220	0,0062	<i>0,0018</i>	0,124	<i>0,009</i>	0,050	<i>0,019</i>	32	5
11/5/2004	13:10	Generalised	4185	0,0450	<i>0,0060</i>	0,353	<i>0,020</i>	0,127	<i>0,024</i>	82	35
5/31/2008	15:00		4281	0,0031	<i>0,0011</i>	0,081	<i>0,007</i>	0,038	<i>0,016</i>	5	0,6
5/31/2008	17:00	Generalised	4264	0,0030	<i>0,0010</i>	0,079	<i>0,006</i>	0,037	<i>0,015</i>	4	0,5
11/2/2008	17:22		4379	0,0099	<i>0,0021</i>	0,151	<i>0,010</i>	0,066	<i>0,019</i>	51	11
11/2/2008	23:09		5373	0,0142	<i>0,0022</i>	0,195	<i>0,011</i>	0,073	<i>0,015</i>	57	14
11/3/2008	06:47		5228	0,0132	<i>0,0021</i>	0,176	<i>0,010</i>	0,075	<i>0,016</i>	59	15
11/3/2008	14:37	Cevenol	4759	0,0093	<i>0,0017</i>	0,136	<i>0,009</i>	0,068	<i>0,017</i>	54	12
11/3/2008	23:55		4604	0,0113	<i>0,0016</i>	0,137	<i>0,008</i>	0,083	<i>0,017</i>	64	18
11/4/2008	07:51		4233	0,0084	<i>0,0015</i>	0,124	<i>0,009</i>	0,068	<i>0,017</i>	54	12
11/4/2008	15:51		4022	0,0055	<i>0,0012</i>	0,111	<i>0,008</i>	0,049	<i>0,015</i>	30	5
2/7/2009	12:37	Generalised	4777	0,0151	<i>0,0022</i>	0,134	<i>0,009</i>	0,113	<i>0,023</i>	77	29
11/5/2011	11:36	Cevenol	4091	0,0216	<i>0,0021</i>	0,221	<i>0,009</i>	0,097	<i>0,014</i>	72	23

Table 4

[Click here to download Table: Table 4.pdf](#)

Part of the Rhone basin	Tributary name	Mean	<i>sd</i>	Min	Max
Northern	Saone River	88	27	39	222
	Iserre River	67	35	33	201
	Ain River	93	33	48	221
	Fier River	44	6	36	66
Southern west bank	Aigues River	128	70	53	373
	Ouveze River	154	80	48	378
	Drome River	136	52	59	252
	Durance River	108	47	41	358
Southern right bank	Gard River	51	10	41	80
	Ceze River	47	10	38	99
	Ardeche River	56	14	39	118

Supplementary material for on-line publication only

[Click here to download Supplementary material for on-line publication only: Supplementary information.pdf](#)